AIAA SciTech Forum
6-10 January 2020, Orlando, FL
AIAA Scitech 2020 Forum

10.2514/6.2020-2041



# Development of a Transverse Low-Turbulence Gust Generator in a Wind Tunnel

David A. Olson,* Ahmed M. Naguib,† and Manoochehr M. Koochesfahani‡
*Michigan State University, East Lansing, Michigan, 48824*

**This work demonstrates the viability of a novel transverse-gust generator that is capable of producing a controllable time-varying gust without increasing the turbulence level within a large region of the flow facility. The new gust generator concept is based on the utilization of a vortex-generator array (*VGA*) along one of the walls of a facility's test section at a given streamwise location. Using such a device, a step-like and a sinusoidal gust with an amplitude of 5.7% are demonstrated experimentally in a wind tunnel. A simplified vortex-array model is shown to be a useful tool for the design of the new gust generator.**



## I. Nomenclature

| | | |
|---|---|---|
| $AR$ | = | aspect ratio |
| $b$ | = | airfoil span |
| $c$ | = | airfoil chord |
| H | = | height of test section |
| $Re_c$ | = | chord Reynolds number; $U_\infty c/\nu$ |
| $U_\infty$ | = | freestream velocity |
| $u$ | = | streamwise flow velocity component |
| $VG$ | = | vortex generator |
| $VGA$ | = | vortex generator array |
| $v$ | = | transverse flow velocity component |
| W | = | width of test section |
| $w$ | = | spanwise flow velocity component |
| X | = | streamwise coordinate |
| Y | = | cross-stream or transverse coordinate |
| Z | = | spanwise coordinate |
| $\alpha_{VG}$ | = | angle of attack of the vortex generators |
| $\Delta_{VG}$ | = | cross-stream spacing of the vortex generators |
| $\nu$ | = | kinematic viscosity |

## II. Introduction

A steady uniform freestream condition is typically employed when evaluating the aerodynamic performance of airfoils. However, there are numerous situations when an airfoil must perform in a more complex flow environment. While the interaction of an airfoil with a transient event (such as a gust) has long been considered, transverse (or vertical) gusts (see Fig. 1 for illustration) have been addressed in fewer studies as they are harder to create experimentally (e.g. see discussions in [1] and [2]). However, the importance of transverse gusts is reflected in a range of recent studies [1-4]. In some of these works, Perrotta and Jones [1] utilize a *steady* water jet in a tow tank to create a transverse gust, while Smith et al. [3] employ a blower assembly to create a *step-like* transverse gust in a wind tunnel while operating at a low freestream speed (1.5 m/s). Even though both of these systems create a strong transverse gust (up to 40% of freestream), they also have large turbulent fluctuation levels about their mean gust velocity (10-20% of freestream).

This study seeks to evaluate a novel transverse gust generation device that introduces *unsteady* gusts into a flow facility while maintaining low turbulence fluctuation levels and has a high degree of controllability in terms of the

* Research Associate, Mechanical Engineering, 1449 Engineering Research Ct A109, East Lansing, MI 48824, AIAA Member.
† Professor, Mechanical Engineering, 1449 Engineering Research Ct C128, East Lansing, MI 48824, AIAA Associate Fellow.
‡ Professor, Mechanical Engineering, 1449 Engineering Research Ct A131, East Lansing, MI 48824, AIAA Associate Fellow.

magnitude, the duration, and the time history of the gust. This design differentiates itself substantially from those in the literature and will be useful in separately considering different attributes of transverse gusts.

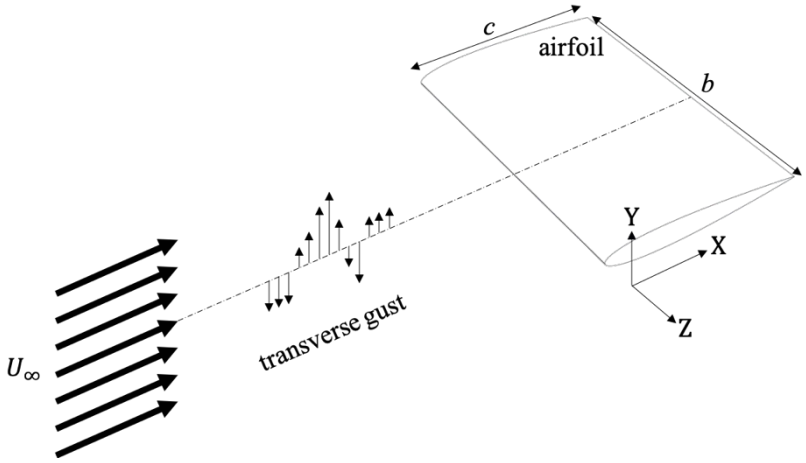


**Fig. 1 Illustration of problem with an airfoil whose chord line is aligned with the freestream (X) direction and whose spanwise coordinate is Z. The freestream velocity is shown to be uniform in the transverse and the spanwise direction. An unsteady transverse gust is shown to act in the (Y) direction.**

## III. Gust Generator Design and Model

The design of the transverse gust generator consists of an array of small vortex generators mounted on one wall of the test section, as shown in Fig. 2. Each vortex generator ($VG$) is a small NACA 0012 airfoil whose tip is a body of revolution. A slider (shown in gold in the bottom of Fig. 3) links all of the vortex generators together such that they can be actuated by a centralized pitch motor. The flow is minimally disturbed when the $VG$s are at zero angle of attack, however, when the $VG$s are pitched to a non-zero angle of attack, a tip vortex forms from each $VG$ (as indicated by the red arrows in Fig. 2 and Fig. 3). The induced velocity field from this array of streamwise vortices constitutes the transverse gust in the central (core) region of the test section. The angle of attack of the $VG$s is the mechanism to change the strength of the tip vortex, and therefore, the strength of the gust. In addition, by dynamically changing the angle of attack, it is possible to control the duration and the waveform of the gust.

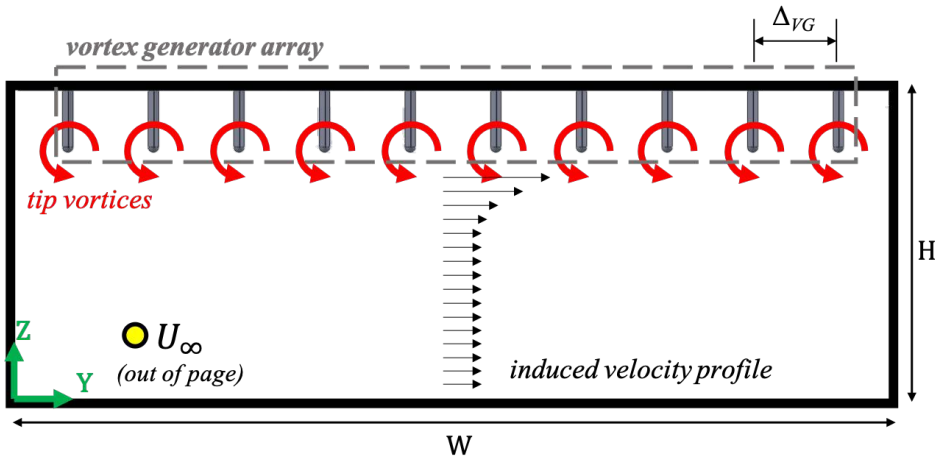


**Fig. 2 Cross-sectional (end) view of the test section where the freestream is out of the page.**

While the fluctuation in the streamwise and transverse velocity components is expected to increase at the center of each tip vortex, the flow away from the center of the vortex cores should remain steady with little fluctuations other than the baseline freestream turbulence. This yields a large portion of the test section where a transverse gust can be introduced into the flow facility without impacting the freestream turbulence level.

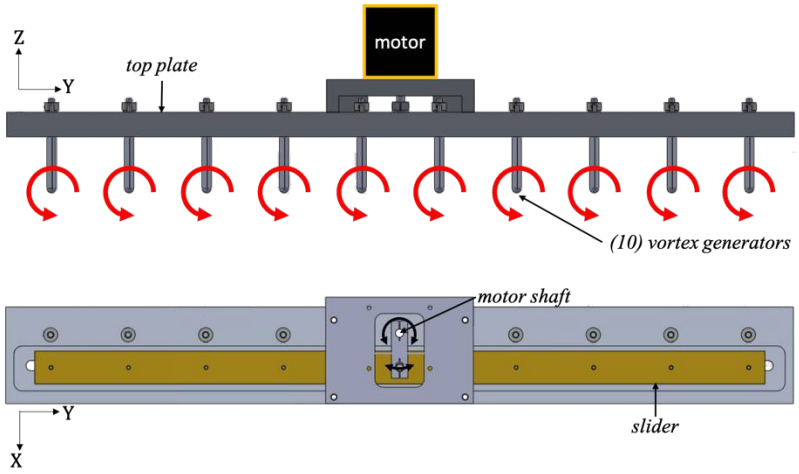


**Fig. 3 Two-view drawing of the gust generator. End view (top) of the vortex generator array. Top view (bottom) does not include the motor to show the motor linkage to the slider (gold). Red arrows indicate vortex sign.**

The tip vortex from an airfoil vortex generator, as studied by Wendt [5-9] and others, has been shown to be modeled satisfactorily by the Lamb-Oseen vortex to capture much of its streamwise evolution. The empirical models developed in the parametric study of Wendt [8] for the circulation and the peak vorticity are used in initial design studies of the current *VG*s. The semi-empirical model takes into account the airfoil's chord, aspect ratio, angle of attack, and the ratio of the span to boundary layer thickness. Multiple vortex generators are modeled through superposition. For simplicity, each tip vortex is modeled as infinite vortex filament with a Gaussian vorticity distribution, whose circulation and peak vorticity are taken from the empirical models. The effect of *all* vortices in the array, including their associated mirror images with respect to all of the walls of the test section, is accounted for using the Biot-Savart law. Only two of the infinite layers of image vortices is included in the design calculations. The effect of additional layers is expected to be negligibly small. Furthermore, the vortex pattern is assumed to be 2D; i.e. the model excludes both the streamwise evolution of the individual vortices and the vortex pattern evolution via inter-vortex interactions. The no-slip viscous boundary layer on the walls are also not taken into account in the calculation.

An initial parametric study was conducted using the above model to consider the effect of the aspect ratio, the chord length, the transverse spacing, and the number of the vortex generators. In Fig. 4 (a-c), a color map of the transverse velocity is shown for 1, 5, and 9 vortex generators whose chord is $c = 80\,mm$, with an aspect ratio $AR = 0.73$, transverse spacing of $\Delta_{VG} = 0.75c$, and an angle of attack $\alpha_{VG} = 16°$. The transverse-velocity profiles normalized by their respective centerline velocity ($v_{cl}$) are extracted at the bottom of the test section and at $\mathrm{Z/H} = 0.5$ and are shown in Fig. 4 (d). Fig. 4 (e) shows the transverse velocity profiles at the center of the test section ($\mathrm{Y/W} = 0.5$). Referring to Fig. 4, as the number of vortex generators increases, the transverse extent of a nominally uniform velocity region increases, and the magnitude of the induced velocity also increases with increasing number of vortex generators. The increase in the transverse velocity is less significant between 5 and 9 *VG*s compared to the initial increase moving from 1 to 5 *VG*s. The increasing number of *VG*s primary effect is to improve the uniformity in the test section (both in the Y and Z directions). While not shown, further increase in the induced transverse velocity and improvements in the associated uniformity can be realized by decreasing the inter-vortex spacing. However, as the spacing between the vortices decreases, small variation in the characteristics of the vortices in practical implementation could lead to

entanglement of neighboring vortices, via the vortex-vortex interactions, which are not accounted for in the present model. This in turn deteriorates the overall uniformity of the associated gust.

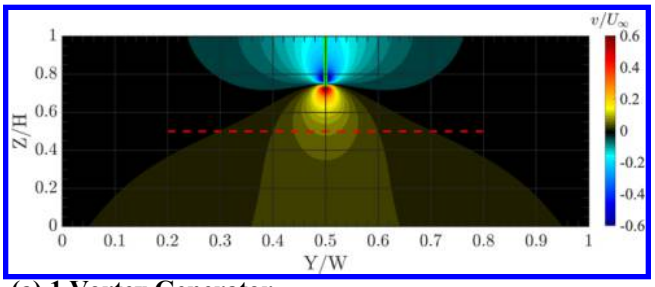


**(a) 1 Vortex Generator**

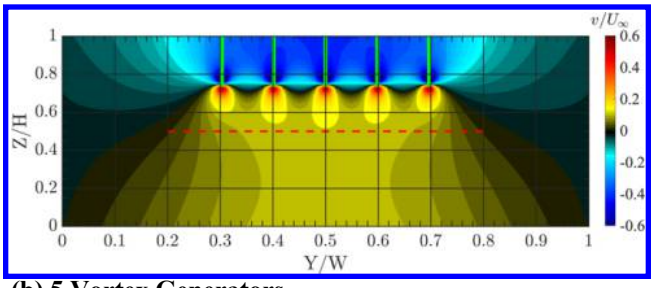


**(b) 5 Vortex Generators**

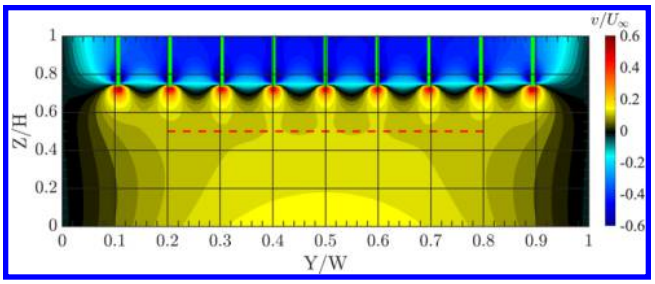


**(c) 9 Vortex Generators**

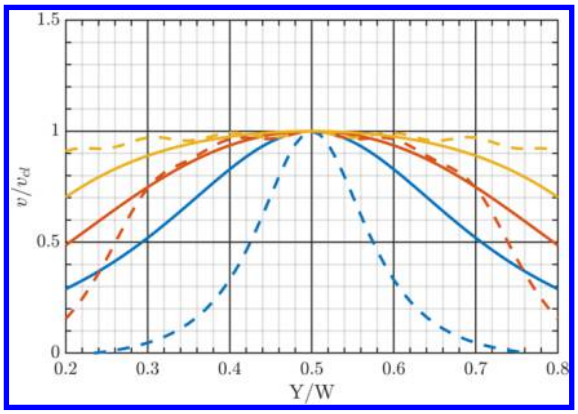


**(d) Normalized Velocity Profiles at Z/H=0.5, Z/H=0**

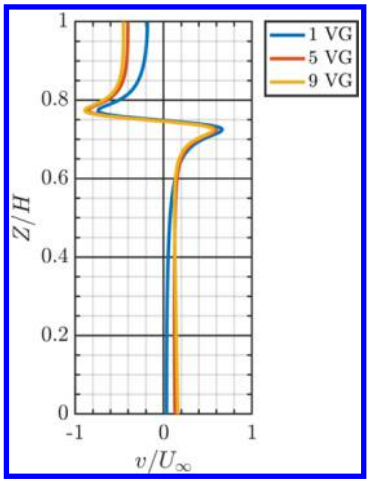


**(e) Velocity Profile at Y/W=0.5**

**Fig. 4 Flooded contours of the transverse velocity for 1 (a), 5 (b), and 9 (c) vortex generators. (d) Profiles of transverse velocity extracted at Z/H=0.5 (broken line) and Z/H=0 (solid line) with the color indicating the number of vortex generators as given in the legend of (e), where each profile has been normalized by the velocity at the centerline of Y/W=0.5. (e) Transverse velocity profiles extracted at Y/W=0.5.**

Based on the above analysis and the physical size of the test section, a design utilizing 10 vortex generators with a chord length $c = 80\ mm$, an aspect ratio $AR = 0.73$, a transverse spacing $\Delta_{VG} = 0.75c$, and an angle of attack $\alpha_{VG} = 16°$ is considered for experimental evaluation. The transverse velocity computed for this configuration over a domain matching the test-section size of the experiments is shown in Fig. 5. The black broken line in the figure outlines a central core region of the test section, where the gust is nominally uniform. This region's extents are $0.4 \leq$ Y/W $\leq 0.6$ and $0.05 \leq$ Z/H $\leq 0.5$. The average transverse velocity in this region is 14% of $U_\infty$ with a spatial variation (root-mean-square, *rms*) of less than a 1.2% of $U_\infty$.

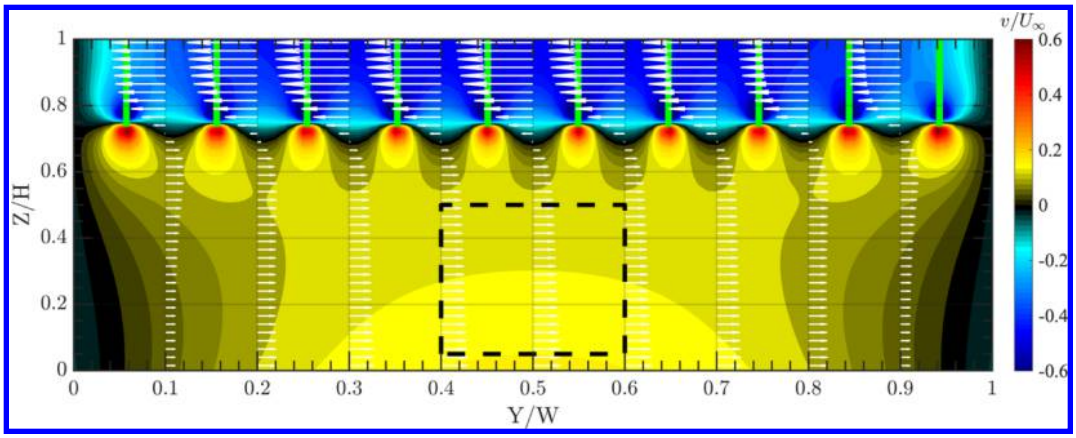


**Fig. 5 Flooded contour map of the transverse velocity in the test section for a vortex generator array consisting of 10 vortex generators (indicated by green lines at the top of the figure). The black broken line encircles the nominally uniform gust domain, and the white vectors show the transverse component at selected locations.**

## IV. Experimental Methods

Experiments are performed in an open-circuit wind tunnel, with test section cross section of 61 cm × 61 cm and a length of 183 cm, located at the Flow Physics and Control Laboratory at Michigan State University. The test section is divided by a false ceiling with the upper section used for instrumentation and the lower section, with a height of 21.6 cm, as the primary flow section. A diagram of the test section is shown in Fig. 6, while a more complete description of the setup can be found in Hamedani et al. [10].

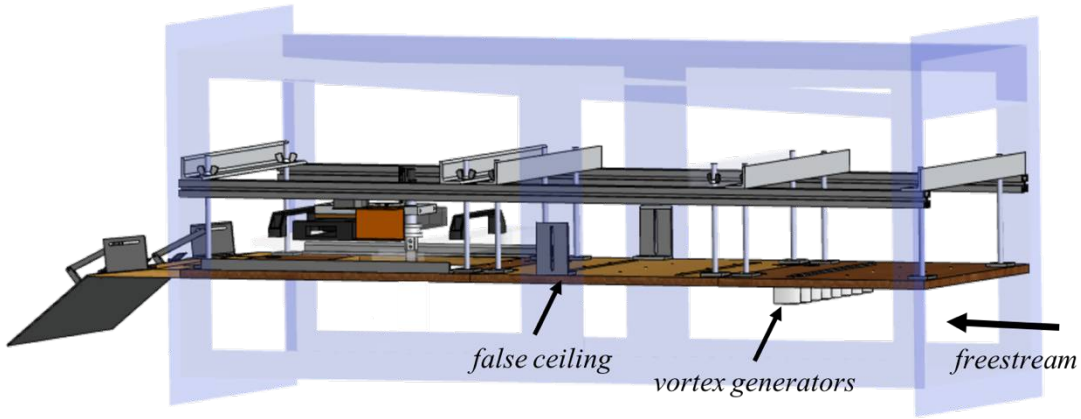


**Fig. 6 Drawing of the test section with the vortex generator array installed in the false ceiling on the upstream side of the test section (flow is right to left).**

The flow field is characterized downstream of the vortex generator array (gust generator) utilizing an X-wire probe. The hot wires were made from 5 μm-diameter tungsten with a sensing length of 1 mm (0.0125$c$). The corresponding sensing volume is approximately 1 mm$^3$. The probes are oriented to measure the streamwise and cross-stream (gust) velocity components; $u$ and $v$ respectively. Each wire is connected to a single-channel of a TSI IFA-300 constant temperature anemometer and are operated at an overheat ratio of 0.6. A 1 kHz low-pass filter is applied onboard of the anemometer while the output voltage of each wire is acquired at 2 kHz on a National Instruments PCI-6034E 16-bit DAQ system. The wires are calibrated against a pitot tube and a cosine yaw dependence of the wires is used with the measured wire orientations relative to the test-section walls. The wire response is fitted to King's law and the temperature compensation method of Hultmark and Smits [11] is applied to correct for temperature variation within

the wind tunnel during measurements, which was typically within 2° C. Measurement uncertainty due to hot-wire calibration drift is ±2% for the results presented herein.

Measurements are performed over the full width and height of the test section. This is accomplished by moving the probe using a stepper-motor-controlled 2D traversing system. The probe is attached to this system using a custom-made holder, which has two mounting locations separated by 280 mm in the y direction. The full height of the test section could not be traversed in a single run, so the holder was modified to allow for a second set of acquisitions to cover the upper and lower parts of the test section. Measurement spacing was 5mm in the Y-direction and 3mm in the Z-direction. After overlapping regions are removed, each measurement consists of nominally 118 x 67 points in the Y and Z directions, respectively. At each measurement location, the velocity is sampled for 18 seconds where the *VGA* is in the "off" configuration for 3 seconds, followed by the actuation of the *VGA* where it remains in the actuated state for 12 seconds and then returns to its "off" configuration. This measurement scheme is sufficient to allow the steady-state velocity to be determined before, during, and after the *VGA* actuation.

The *VGA* actuations considered were: a *step-like* maneuver from $\alpha_{VG} = 0°$ to $\alpha_{VG} = +16°$ (and its return to 0°), and a sinusoidal variation of $\alpha_{VG}$, with an amplitude of 16° and a frequency of 2 Hz. The hot-wire probe outputs are sampled for at least 2.5 seconds under each steady state condition, which corresponds to 312 convective times based on the vortex generator chord length and a freestream velocity of 10 m/s. The resulting random uncertainty in mean-velocity measurements is 0.2% of the freestream velocity.

## V. Results

Several different vortex generator array arrangements with varying chord, aspect ratio, and spacing were initially considered experimentally. Results from characterizing several of these configurations are summarized in Fig. 7, where the transverse velocity profiles extracted at a height of *Z/H*=0.36 are shown across the width of the test section for measurement at 350 mm downstream of the *VGA*. Testing of $c = 60\ mm$ vortex generators shows that increasing the spacing from $\Delta_{VG} = 0.5c$ to $\Delta_{VG} = 1.0c$ greatly improved the uniformity of the velocity across the test section but at the expense of a lower magnitude transverse velocity. It was observed that as $\Delta_{VG}$ decreased, the interactions between neighboring vortices increased, especially at either end of the array, resulting in more complicated vortex patterns and an increasing non-uniformity across the test section. These observations were consistent with the modeling results regarding the effect of the *VG* spacing in increasing the transverse velocity, but since the model did not account for the streamwise evolution of the array, theses initial experiments helped guide the choice of the vortex-generators spacing that would be considered further. A balance between the magnitude of the induced velocity and uniformity was achieved by increasing the chord of the vortex generators to $c = 80\ mm$ and using $\Delta_{VG} = 0.75c$ for the inter-vortex spacing (Fig. 7). The final *VGA* configuration consisted of an array of 10 vortex generators to fit as many *VGs* as possible within the available width of the test section.

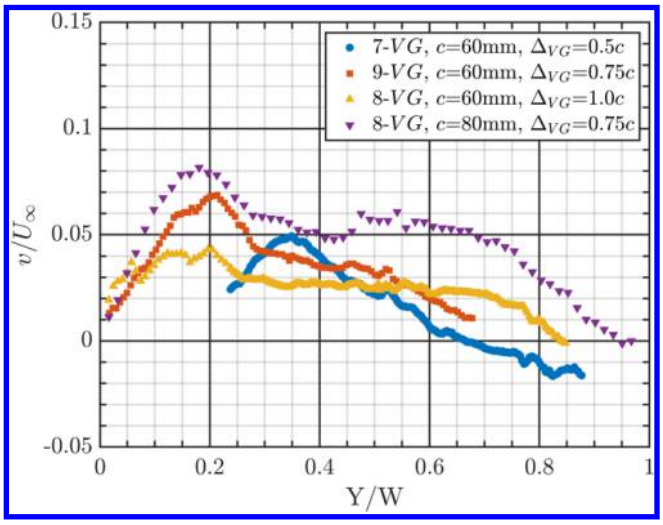


**Fig. 7 Mean transverse velocity profiles extracted at a Z/H=0.36 and streamwise location of 350 mm downstream of the vortex generators for several *VGA* configurations.**

The array of 10 *VGs* with a chord length $c = 80\ mm$, a span of 58 mm (for an aspect ratio of $AR = 0.73$), and a $y$-spacing of $0.75c$ is characterized using measurements conducted at X=650 mm downstream of the trailing edge of the *VGA* (when $\alpha_{VG} = 0°$). The *VG* Reynolds number is $Re_c = 5.2 \times 10^4$. Figure 8 shows the mean transverse-velocity change between the "off" and "actuated" steady-state conditions for the *step-like* actuation from 0° to $\alpha_{VG} = +16°$. The figure is used to analyze two aspects of the gust generator's performance: (I) the behavior of the vortices, and (II) the cross-stream mean-flow generated by the static *VGs*. First, we observe that all except the outboard vortices retain the intended formation of a wall-parallel array of vortices. Considering the induced velocity on the outboard vortices, it is expected that the right-most vortex will move towards the top wall, and the left-most vortex will move away from the same wall with downstream distance, which is clearly seen in the data. Once the left-most vortex has moved away far enough, the next inboard vortex is expected to start moving away from the wall, which is also observed. On the other hand, the inboard vortices are stabilized by the opposing upwash/downwash effect of their neighboring vortices immediately to the left and to the right, and hence these vortices remain in a well-behaved pattern. In addition to the undesirable up and down movement of the end vortices, the entire vortex array shifts leftward as it convects downstream. This expected behavior, due to the influence of the image vortices (i.e. wall presence), is small enough (less than $\Delta_{VG}$) that it should not influence the quality of the cross-stream flow in the central portion of the test section.

Turning attention to the characteristics of the steady transverse flow produced in the test-section core region, which is shown by the broken red line of Fig. 8. The average velocity over this central 20% of the test section width and 55% of its height is 5.7% of $U_\infty$ with spatial *rms* variation over this domain of less than 0.7% of $U_\infty$. The uniformity of the transverse velocity is more easily assessed in Fig. 9, where the velocity profiles along the boundary of this region are shown. There is more *rms*-deviation across the upper and lower boundaries (12.0% and 12.1%), Fig. 9 (a), compared to those along the sides of the boundary (6.6% and 4.3%), Fig. 9 (b). Some of the deviation across the test section width is likely due to the extent at which the outboard vortices have started to deviate from the wall parallel arrangement, so it is likely that the uniformity will improve at streamwise positions closer to the *VGA*.

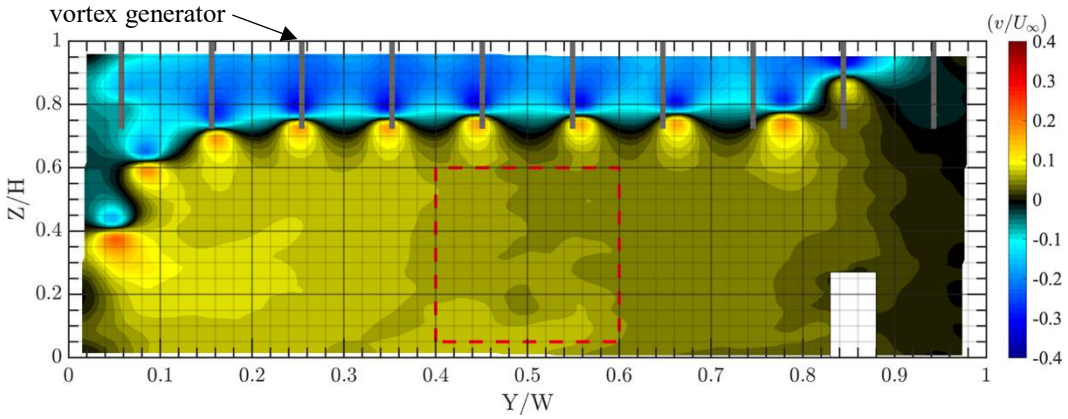


**Fig. 8 Mean transverse velocity at a distance of X=650 mm downstream of the vortex generator array.**

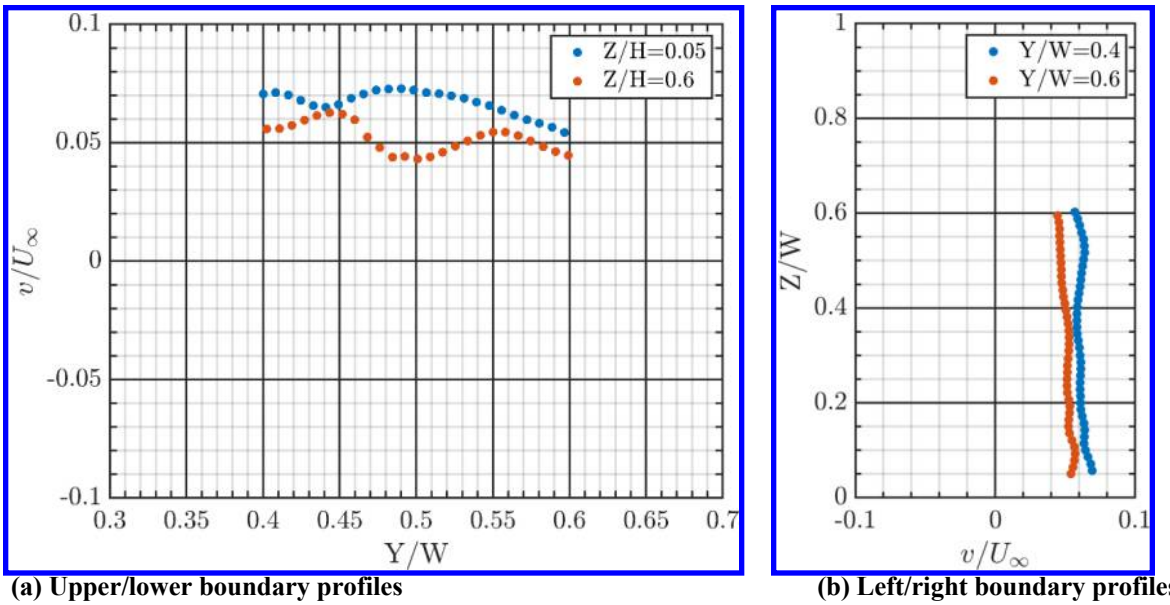


**(a) Upper/lower boundary profiles** **(b) Left/right boundary profiles**

**Fig. 9 Mean transverse velocity profiles extracted at the (a) upper/lower, and (b) left/right bounds of the nominally uniform region.**

Compared to the model prediction in Fig. 5, the measured results have a lower transverse-velocity magnitude (by ~60%). Two major sources that could be causing this discrepancy are: (1) inaccuracy in the characteristics of the tip vortex used in the model (circulation and core radius); (2) not taking various aspects of the real flow into account in the model. These include, the inter-vortex interactions, the no-slip boundary condition at the walls, the streamwise evolution of the entire vortex array, and the streamwise decay of the vortices. The differences observed between the model and the measurements, in terms of the vortex size and the circulation, can be incorporated into the empirical model to further improve the model. In addition, the streamwise evolution of the vortices as they interact with one another can be implemented in the model. Generally speaking, however, notwithstanding the quantitative difference between the experimental data and the model results, the model is a good predictor of the trends in *VGA* performance with changes in the various parameters of the *VGA*, which was the primary function of the model for the gust generator design.

One of the key attributes of the present gust generator is that the generator does not produce turbulent fluctuations in the freestream. This feature is assessed using Fig. 10, where the root-mean-square (*rms*) of both the streamwise and the transverse velocity fields are shown at steady state at the X=650 mm downstream measurement plane for both the baseline condition ($\alpha_{VG} = 0°$), and with the *VGA* actuated to $\alpha_{VG} = 16°$. While we do observe an increase in the fluctuation at the center of the vortices due to actuation, the central region of the test section exhibits little difference. The average fluctuation levels in the aforementioned central region (0.4≤Y/W≤0.6, 0.05≤Z/H≤0.6) are 1.0% and 0.6% of $U_\infty$ for $u_{rms}$ and $v_{rms}$, respectively, for the baseline case. For the actuated case, these fluctuation levels are 1.1% and 0.6% of $U_\infty$ for $u_{rms}$ and $v_{rms}$, respectively, which are practically the same as the baseline case.

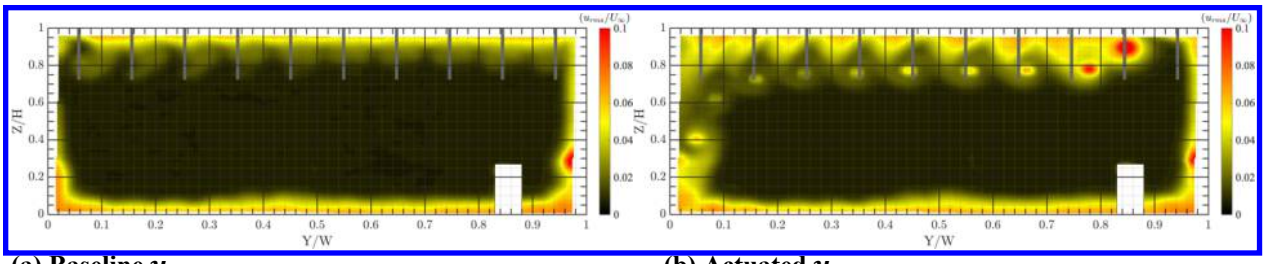


(a) Baseline $u_{rms}$ (b) Actuated $u_{rms}$

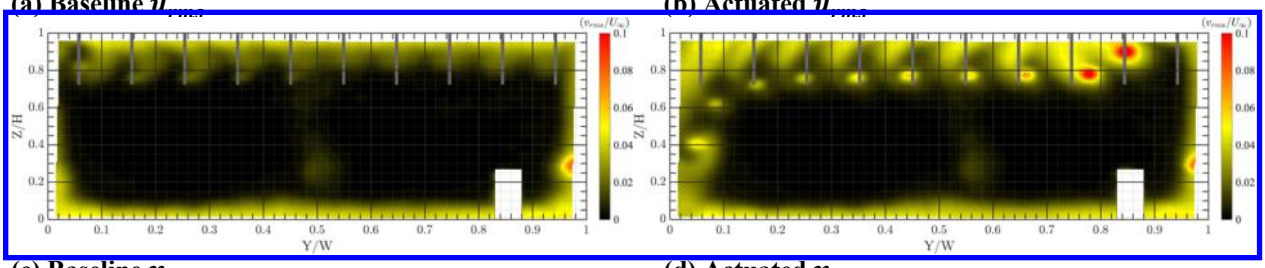


(c) Baseline $v_{rms}$ (d) Actuated $v_{rms}$

**Fig. 10 The *rms* of the streamwise, (a) and (b), and the transverse, (c) and (d), velocity at a downstream distance of X=650 mm downstream of the *VGA* with $\alpha_{VG}$=0°, (a) and (c), and $\alpha_{VG}$=16° (b) and (d).**

Another key attribute of the gust generator's design is the ability to create unsteady gusts. This is demonstrated by considering a *step-like* actuation and a sinusoidal actuation of $\alpha_{VG}$ according to $\alpha_{VG} = 16° \, H(t-3)$, and $\alpha_{VG} = 16° \, \sin 2\pi f t$ (where $H$ is the Heaviside step function). A frequency $f = 2.0 \, Hz$ is used for sinusoidal actuation. The streamwise and transverse velocity components, averaged over the aforementioned central region, are shown versus time in Fig. 11 for both types of actuation. As discussed previously, the step-like actuation yields a transverse velocity of 5.7% of $U_\infty$ during the steady actuation period; we observe here that the transverse velocity increases smoothly to this value with no overshoot/undershoot in ~175ms. There is a slight delay (~60ms) from when the *VGA* is actuated ($t = 3.0$) to when a change in velocity is observed, but this delay is consistent with the convective time over the distance from the *VG* to the downstream measurement location at the freestream velocity. The transverse velocity of the sinusoidal actuation achieves nearly the same magnitude as the step-like motion, with only a slight asymmetry for positive versus negative velocity (which is attributed to friction in the mechanical linkage of the *VGA*).

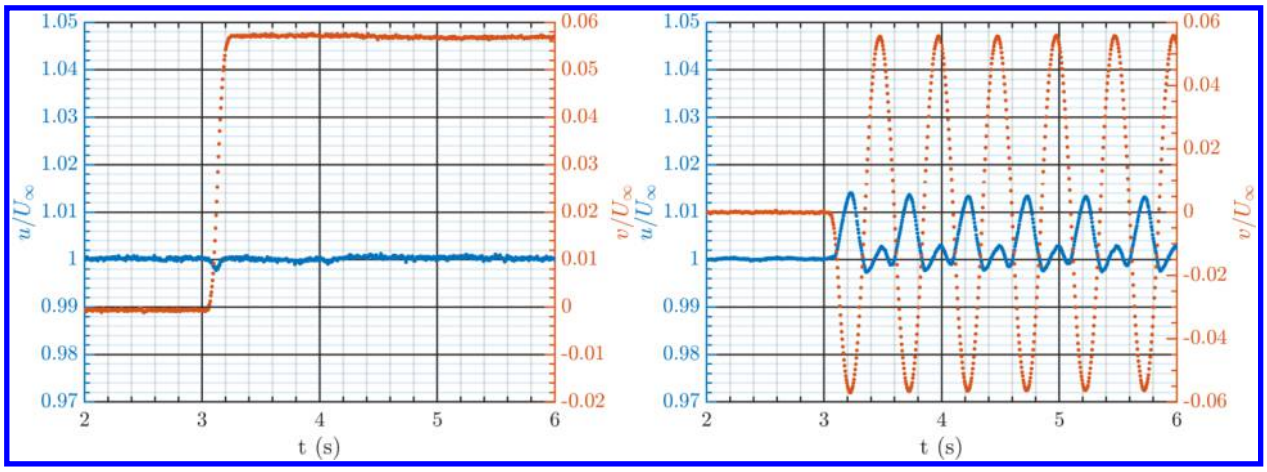


(a) Step-like Gust (b) Sinusoidal Gust

**Fig. 11 The streamwise and the transverse velocity components during the (a) step-like and (b) sinusoidal actuation. Separate axis with corresponding color depicts each of the velocity components.**

The *step-like* actuation shows only a small effect on the streamwise velocity, characterized by a decrease in the velocity during the actuation time by a magnitude of only $0.002U_\infty$. A different behavior is observed in the sinusoidal actuation case, with the streamwise velocity varying between $1.014U_\infty$ and $0.998U_\infty$. The asymmetry in the response is likely a peculiarity with our particular setup. While these changes in streamwise velocity are already small, they could be mitigated by incorporating a streamwise-gust louver system to provide the necessary "anti-gust" placed on the downstream portion of the test section.

## VI. Summary

A novel transverse gust generator has been modeled, designed, and tested. The gust generator consists of an array of vortex generators (*VGA*) mounted to the top wall of a wind tunnel's test section. The primary advantage of the new gust generator over other transverse gust generators is that it can produce a transverse stream with a high degree of uniformity without increasing the turbulent fluctuations in the freestream. Additionally, the generator's concept allows for unsteady gusts (±5.7% of freestream velocity in the present design) to be created. The modeling work has yielded a useful tool that will be improved with the incorporation of empirical information from the various test cases.



## VII. Acknowledgments

This project is funded by ONR grant number N00014-16-1-2760. The views and conclusions contained in this document are those of the authors and should not be interpreted as representing the official policies, either expressed or implied, of ONR or the U.S. Government. The U.S. Government is authorized to reproduce and distribute reprints for Government purposes notwithstanding any copyright notation herein.

## References

[1] Perrotta, G., & Jones, A. R. (2017). Unsteady forcing on a flat-plate wing in large transverse gusts. *Exp Fluids*, *58*, 101. (https://doi.org/10.1007/s00348-017-2385-z)

[2] Corkery, S. J., Babinsky, H., & Harvey, J. K. (2018). On the development and early observations from a towing tank-based transverse wing–gust encounter test rig. Experiments in Fluids, 59(9), 135. (https://doi.org/10.1007/s00348-018-2586-0)

[3] Smith, Z.F., Jones, A.R., Hrynuk, J.T., Micro Air Vehicle Scale Gust-Wing Interaction in a Wind Tunnel, 2018 AIAA Aerospace Sciences Meeting, AIAA SciTech Forum, 2018-0573

[4] Poudel, N., Yu, M., Smith, Z. F., & Hrynuk, J. T., A combined experimental and computational study of a vertical gust generator in a wind tunnel, 2019 AIAA Aerospace Sciences Meeting, AIAA SciTech Forum, 2019-2166. (https://doi.org/10.2514/6.2019-2166)

[5] Wendt, B. J., Reichert, B. A., and Foster, J. D., "The Decay of Longitudinal Vortices Shed from Airfoil Vortex Generators," AIAA Paper 95-1797, June 1995.

[6] Wendt, B. J., and Reichert, B. A., "The Modeling of Symmetric Airfoil Vortex Generators," AIAA Paper 96-0807, Jan. 1996.

[7] Wendt, B. J., and Reichert, B. A., "Spanwise Spacing Effects on the Initial Structure and Decay of Axial Vortex Generators," NASACR 198544, Nov. 1996

[8] Wendt, B. J., "Initial Circulation and Peak Vorticity Behavior of Vortices Shed from Airfoil Vortex Generators," NASA CR 2001-211144, Aug. 2001.

[9] Wendt, B. J., Parametric Study of Vortices Shed from Airfoil Vortex Generators. *AIAA Journal*, Vol. 42, No. 11, 2004, pp. 2185–2195. (https://doi.org/10.2514/1.3672)

[10] Hamedani, B. A., Naguib, A. M., and Koochesfahani, M. M., "Reynolds Number Effect on Lift Characteristics of an Airfoil Translating Across a Non-uniform Approach Flow." 2019 AIAA Aerospace Sciences Meeting, AIAA SciTech Forum, (AIAA 2019-0639) (https://doi.org/10.2514/6.2019-0639)

[11] Hultmark, M., & Smits, A. J., Temperature corrections for constant temperature and constant current hot-wire anemometers. Measurement Science and Technology, 21(10), 2010. (https://doi.org/10.1088/0957-0233/21/10/105404)